Neuron, Vol. 42, 803–815, June 10, 2004, Copyright ©2004 by Cell Press

A Double Dissociation between Hippocampal Subfields: Differential Time Course of CA3 and CA1 Place Cells for Processing Changed Environments

Inah Lee,[1] Geeta Rao, and James J. Knierim*
Department of Neurobiology and Anatomy
W.M. Keck Center for the Neurobiology of Learning and Memory
University of Texas Medical School at Houston
Houston, Texas 77225

Summary

Computational theories have suggested different functions for the hippocampal subfields (e.g., CA1 and CA3) in memory. However, it has been difficult to find dissociations relevant to these hypothesized functions in investigations of the hippocampal correlates of space ("place fields") in freely behaving animals. The current study demonstrates a double dissociation between the shifts in the center of mass (COM) of the place fields that were simultaneously recorded in CA1 and CA3 when familiar cue configurations were dynamically changed over days. The COM of CA3 place fields shifted backward in the first experience of the cue-changed environment, whereas the COM of CA1 place fields did not display the backward shift until the next day. These results support the hypothesis that CA3 plays a key role in the rapid formation of representations of new spatiotemporal sequences, whereas CA1 may be more important for comparing currently experienced sequence information with stored sequences in the CA3 network.

Introduction

The hippocampus plays a critical role in spatial memory as well as episodic memory in humans (O'Keefe and Nadel, 1978; Scoville and Milner, 1957; Vargha-Khadem et al., 1997). Hippocampal pyramidal cells increase their firing rates to represent specific spatial locations (place fields) in an environment, and they are typically inactive in other regions of that environment (O'Keefe and Dostrovsky, 1971; O'Keefe and Nadel, 1978). One of the dynamic properties of the place field is that the center of mass (COM) of the field shifts in an experience-dependent manner; specifically, Mehta et al. (1997, 2000) demonstrated that the COM of place fields in CA1 moved backward relative to the rat's direction of motion when rats traversed a track. Mehta et al. (1997, 2000) suggested that the COM shift reflected the encoding, by synaptic weight changes, of specific spatiotemporal sequences of locations in a well-learned route, as predicted by a number of computational models (August and Levy, 1999; Blum and Abbott, 1996; Koene et al., 2003; Levy, 1989).

In order to fully understand the mechanisms and functional significance of the COM shift phenomenon in CA1, it is essential to investigate the properties of its afferent structures. Differences between the properties of the inputs to CA1 and its outputs can determine whether the phenomenon is generated within CA1 and can lead to the deduction of important principles of information processing in the hippocampus. CA1 receives a large input from the Schaffer collateral system of CA3. A recent study reported a dissociation of the function of the NMDA receptors (NMDARs) in CA1 and CA3 in a spatial working memory task (Lee and Kesner, 2002). Pharmacological blockade of NMDARs in CA3 or CA1 had no effect in a short-term spatial working memory task in a familiar environment. However, the same blockade of NMDARs in CA3, but not in CA1, severely impaired the animal's ability to initially perform the same task in a novel environment. Because the COM shift of CA1 place fields has also been shown to depend on NMDARs (Ekstrom et al., 2001), the COM shift and the processing of novel environments are likely to share a common mechanism involving NMDAR-dependent plasticity. In light of the behavioral data suggesting that NMDAR-dependent plasticity mechanisms in CA3 are necessary for learning on a rapid timescale (Lee and Kesner, 2002; Nakazawa et al., 2003), we hypothesized that the experience-dependent shift in the COM of place fields would occur initially in CA3 when an animal experienced novel configurations of spatial cues in an environment. As the animal gained more experience with the changed cue configurations, the shift in the COM would eventually occur in CA1 as well. To test this hypothesis, we recorded place fields simultaneously from CA1 and CA3 of the dorsal hippocampus in freely moving rats in a controlled environment, in which the relationships among cues changed dynamically across behavioral sessions over days. Sessions with a familiar cue configuration were interleaved with sessions in which the relationships among those familiar cues were altered.

We report here a double dissociation between CA1 and CA3 with respect to the shift in the COM of their place fields. That is, the COM of CA3 place fields shifted backward with experience when novel cue configurations were introduced for the first time on day 1, whereas the COM of CA1 place fields showed no backward shift in the same condition. In contrast, a reversed pattern was observed between the two subfields on subsequent presentations of the new cue configurations on later days. The results support the previous behavioral data with respect to the time course of NMDAR-dependent processes in CA1 and CA3 (Lee and Kesner, 2002, 2004; Nakazawa et al., 2003; Shimizu et al., 2000) and provide direct physiological evidence that plasticity in the CA3 network is specialized to underlie learning on a rapid timescale (as is necessary for episodic memory), whereas plasticity in the CA1 network occurs after a delay and may be involved in the comparison of present experiences with stored representations of previous experiences in the CA3 network.

Results

Place fields of CA1 and CA3 were monitored using multiple tetrodes while 14 rats ran on a circular track located

*Correspondence: james.j.knierim@uth.tmc.edu
[1]Present address: Center for Memory and Brain, Boston University, 2 Cummington Street, Boston, Massachusetts 02215.

in a cue-controlled environment, in which multiple distal cues were available along the walls and on the floor, and distinct local cues were present on the track (Figure 1A). Place cells were simultaneously recorded from CA1 and CA3 in some of the animals ($n = 6$; Figure 1B), whereas cells were recorded from either CA1 ($n = 7$) or CA3 ($n = 1$) in the others. The CA3 electrodes were typically lowered to the pyramidal cell layers that are located in the distal or middle portion of CA3, distal to the hilar area (below the CA1 or CA2 cell layers or at the lateral tip of the dorsal hippocampus; Figure 1B). When CA1 cells were recorded simultaneously with CA3 cells, the CA1 electrodes targeted the proximal or middle CA1 cell layers (farther from the subiculum; Figure 1B), as the anatomical literature shows that the distal and middle CA3 regions typically send their Schaffer collateral axons to the proximal and middle CA1 regions, respectively (Ishizuka et al., 1990). Of the cells that were recorded from the tetrodes, only those that were unambiguously assigned to either CA1 or CA3 were used for further analysis (e.g., cells in CA2 or the hilar area were not used).

During pretraining, each animal was familiarized to the environment in which the relationships among cues remained constant (standard session; Figure 1A). Afterward, five experimental sessions were given daily for 4 consecutive days; on each day, three standard sessions were interleaved with two mismatch sessions, in which local cues on the track surface were rotated counterclockwise, and distal cues were rotated clockwise to cause a predetermined amount of mismatch between distal and local cues (i.e., 45°, 90°, 135°, or 180°; Figure 1A). For each session, the rats ran 15 laps in a clockwise direction for a food reward that was placed at arbitrary locations on the track. We examined the place cells in dorsal CA1 and CA3 over 4 consecutive days. Among all the recorded pyramidal cells, only the cells with stable unit isolation across sessions were included to compare the two subfields; the recording was considered stable when the firing patterns of cells were maintained between pre- and postexperimental sleep sessions (Figure 1C). In addition, units were analyzed only if they met criteria for spatially selective firing on the track (spatial information score ≥ 0.5 with $p \leq 0.01$; number of spikes ≥ 50; spatial information score was calculated following Skaggs et al., 1993, 1996). On average, 6.8 cells from CA1 (range, 1–25) and 6.4 cells from CA3 (range, 1–19) met the stability and spatial firing criteria for each session. The data analyses were limited to the first standard and the first mismatch sessions of each day to exclude possible confounding interactions between different cue configurations in the later mismatch sessions of the day (for later sessions, see Supplemental Figure S1 at http://www.neuron.org/cgi/content/full/42/5/803/DC1). The mismatch sessions with different mismatch angles were combined together in the analysis, as there were no significant differences among those sessions. Furthermore, the patterns of partial remapping that were previously reported in the current paradigm (Knierim, 2002) were not systematically related to the differential COM shift between CA1 and CA3 that is described below.

Lap-by-Lap COM Shift in CA3 and CA1

For each cell, the COM of its firing field was calculated for the combined firing from all 15 laps in the session (session-based COM). The session was then divided into individual laps, and the COM of the place field on each specific lap (lap-based COM) was calculated and subtracted from the session-based COM to generate a measure of the shift in the COM on each lap (ΔCOM; Figure 2A). The ΔCOM was examined in CA1 and CA3 across 4 days for each standard and mismatch session (each session will henceforth be abbreviated as D1-STD-CA1, for example, to denote the data from the CA1 place fields that were recorded in the standard session on day 1). To first compare the overall magnitude of COM shifts in the standard and mismatch environments, we examined the COM shift for all data combined over 4 days (Figure 2B). There was a gradual COM shift in CA1 in the standard as well as in the mismatch sessions, as the slopes of the regression lines were significantly negative in both sessions (p values < 0.0001). Although there was an initial forward shift of the COM of CA1 place fields between laps 1 and 2 in the standard session, the COM shifted steadily backward from laps 2 to 15. (The reason for the initial forward shift is not clear, and it may reflect statistical fluctuation; nonetheless, the backward shift for the remaining laps is clear and statistically significant.) The amount of maximum COM shift (4.6°, or 2.6 cm, between lap 2 and lap 15; Figure 2B) in CA1 in the standard sessions was 7% of the average, session-based, CA1 place field size (66°), which is similar to the amount of COM shift (1.4 cm, or 5% of the population average place field) that was originally reported by Mehta and colleagues (see Figure 1C in Mehta et al., 1997, or Figure 3 in Mehta and McNaughton, 1997). In contrast to CA1, no COM shift was observed in CA3 across laps in the standard sessions, as the slope of the regression line was not significantly different from 0 ($p > 0.5$). The pattern of results in the mismatch sessions was quite different, however. The backward shift in CA1 was greater in the mismatch sessions (note the difference in the ordinate scales between STD and MIS in Figure 2B), as was previously shown by Knierim (2002), and the present results include some of the data from that study. More importantly, there was a significant COM shift across laps in CA3 in the mismatch sessions ($p < 0.0001$; Figure 2B). The slopes of the regression lines between the standard and mismatch sessions (Figure 2B) were significantly different in CA3 ($p < 0.0001$; ANCOVA), but not in CA1 ($p > 0.1$), although the same trend is observable in CA1. In sum, the backward COM shift occurred in CA1 in the familiar environment, as previously reported by Mehta et al. (1997, 2000), but not in CA3. However, the altered environments produced shifts in the COM in both subfields to a greater degree.

Although both subfields developed similar amounts of backward COM shifts across laps in mismatch sessions when the data were combined over 4 days (Figure 2B), the time course with which those COM shifts occurred was different in CA1 and CA3; specifically, a double dissociation between CA1 and CA3 was found in the COM shifts for the mismatch sessions on day 1 and the following days. The COM in CA3 shifted backward when the animal experienced a mismatch session for the first

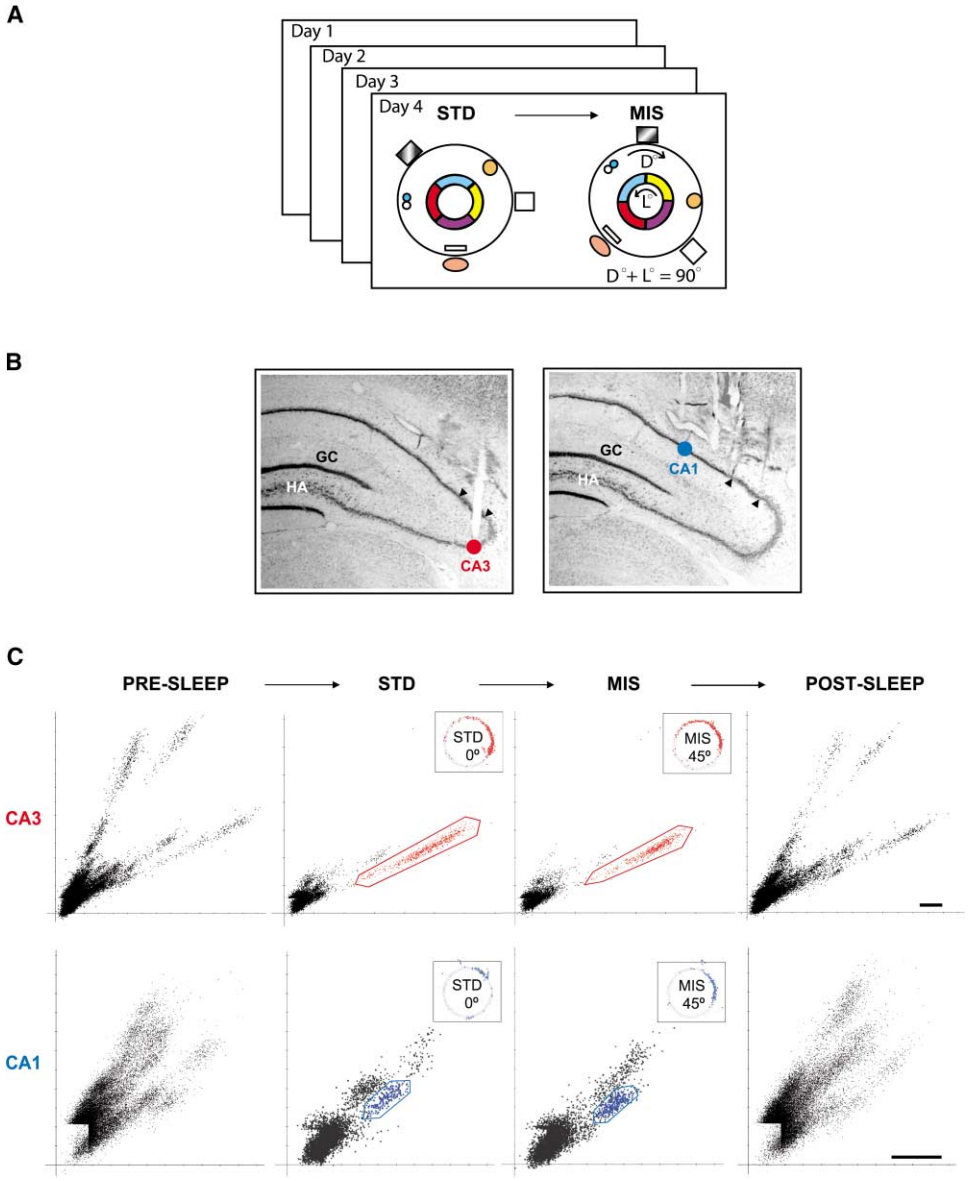

Figure 1. Experimental Paradigm

(A) Illustration of behavioral paradigm and apparatus. The circular track at the center was composed of four different textured surfaces (local cues; denoted by different colors on the track), each covering one-quarter of the track. Surrounding the track were various visual cues, either hanging on the curtain (the three cues shown outside the outer circle; the curtain is not shown for simplification) or standing on the floor (the three cues inside the outer circle). During pretraining, the relationships between the local and distal cues were maintained constant ("standard session" or STD). In the recording sessions, the standard session was followed by a "mismatch session" (MIS) in which the track was rotated counterclockwise, and all the distal cues were rotated clockwise by the same amount (denoted as L° for local cues and D° for distal cues). This double rotation produced a predetermined amount of mismatch between the local and distal cues (90° in this example). On each of 4 days, three standard sessions were interleaved with two mismatch sessions (of different mismatch angles). Only the first standard and mismatch sessions of each day were analyzed and shown here.

(B) Examples of tetrode locations in CA3 and CA1. Different septotemporal levels of histological sections of the dorsal hippocampus (within a subject) are shown. GC, granule cell layer; HA, hilar area. Note that the CA3 recording probe targeted the distal CA3 region after passing through CA2, and the CA1 recording probe targeted the proximal or middle portion of CA1. Arrowheads denote the boundaries of CA2.

(C) Examples of single units that were simultaneously recorded from CA1 and CA3 and their place fields in different cue conditions. Raw data came from the tetrodes shown in the histological sections (B); each point represents the peak amplitude (μV) of a spike recorded on two of the channels of the tetrode (scale bars, 100 μV). An example of a unit from the CA3 tetrode (shown as a red cluster of dots with a red cluster boundary) and its place fields in the standard and the following mismatch sessions are presented (insets; 45° mismatch angle in this example). Shown below are the place fields (insets; blue) from a CA1 unit that was recorded simultaneously with the CA3 unit. "PRE-SLEEP" and "POST-SLEEP" indicate raw data that were collected during sleep before and after the behavioral sessions to confirm the stability of recording during behavioral sessions.

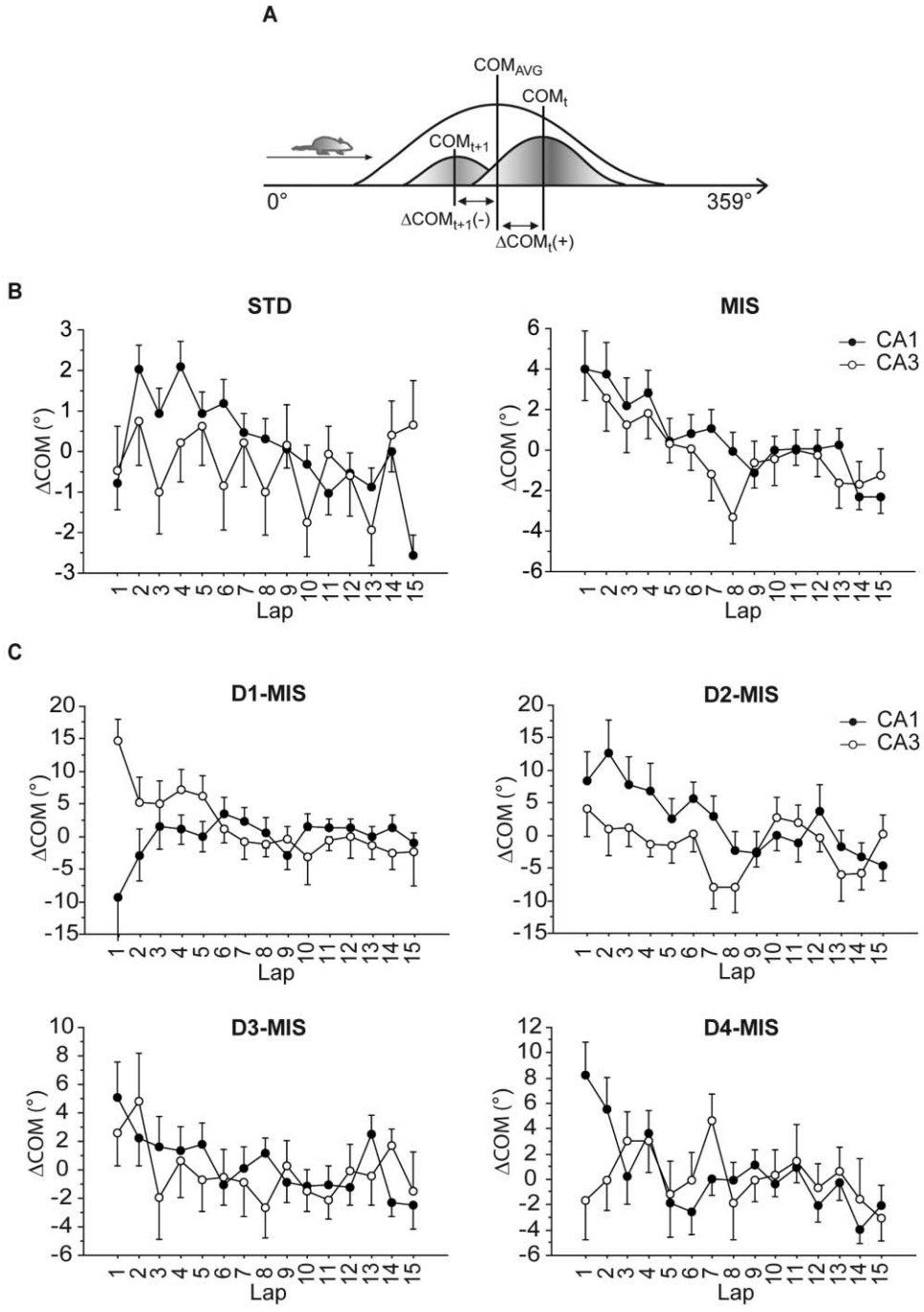

Figure 2. Center of Mass Shift

(A) Illustration of the calculation procedure for the difference (ΔCOM in degrees) between a lap-based COM (COM_t or COM_{t-1}) and the COM of the session-based, average place field (COM_{AVG}). When the lap-based COM (COM_t) is past the COM_{AVG}, the ΔCOM is positive (ΔCOM_t), whereas the ΔCOM is negative (ΔCOM_{t-1}) when the lap-based COM (COM_{t-1}) is ahead of the COM_{AVG} relative to the direction of movement of the rat.

(B) Lap-based ΔCOM of the CA1 and CA3 place fields in the standard (STD) and the mismatch (MIS) sessions (4 days' data were combined). Note the difference in the scales of the ordinates in STD and MIS and the bigger shifts in the COM in the mismatch sessions; the ordinate scale of STD was increased relative to that of MIS to emphasize the comparable shift in the COM that occurred in the standard sessions in CA1 to the COM shift that was reported previously (Mehta et al., 1997, 2000).

(C) Lap-based ΔCOM of the CA1 and CA3 place fields in the mismatch sessions across 4 days (D1-MIS to D4-MIS). The ordinate scales for D3-MIS and D4-MIS are different from those of D1-MIS and D2-MIS for better presentation of the trends in the data.

Table 1. A Comparison between ΔCOM of the First and the Last Laps in CA1 and CA3

	Lap 1		Lap 15		Difference	Linear Field Size (°)		Percent Shift Relative to Linear Field Size
CA1-D1-MIS	8.8	7.0	1.0	1.4	7.8	98.5	6.0	7.9%
CA3-D1-MIS	14.8	3.1	2.3	5.0	17.1	127.5	17.6	13.4%
CA1-D2-MIS	8.0	4.1	4.3	2.2	12.3	104.4	8.3	11.8%
CA3-D2-MIS	3.9	3.9	0.3	2.7	3.6	152.1	12.6	2.4%

time on day 1, whereas the COM remained unchanged in CA1 in the same condition (Table 1; D1-MIS in Figure 2C). The effects in CA3 and CA1 reversed from day 2 (D2-MIS-CA1) onward, however, as the COM shifted backward in CA1 and showed no significant shift in the same condition in CA3 (Table 1; Figure 2C). An ANOVA with the subfield (CA1 versus CA3), day (1–4), and lap (1–15) as three between-group variables showed a significant triple interaction among those variables (subfield day lap; $p < 0.001$). A regression analysis indicated that the slope of the regression line (lap number ΔCOM) was significantly different from 0 in D1-MIS-CA3 ($p < 0.0001$), but not in CA1 in the same condition ($p > 0.1$). The slopes of the regression lines were not different from 0, however, in CA3 after day 1 between the lap number and ΔCOM (p values > 0.1). Conversely, the slopes of the regression lines were significantly negative in CA1 in the mismatch sessions from day 2 onward (p values < 0.001). Furthermore, the slopes of the regression lines for individual units were calculated and compared across days and subfields (see Supplemental Figure S2 at http://www.neuron.org/cgi/content/full/42/5/803/DC1). The mean slopes were significantly different from 0 in CA3 only on day 1 and in CA1 only on days 2–4. Although a number of CA1 cells showed a negative slope on day 1, these cells were cancelled by other cells showing a positive slope, resulting in the overall lack of a significant backward shift of the population in CA1-D1-MIS (Figure 2C).

The ΔCOM data can be considered as time series data, since successive values in the data represent consecutive measurements that were taken at equal intervals (i.e., each lap). As most other statistics assume that the samples of observations are randomly obtained, a more accurate description of the time-dependent trend in the ΔCOM data may be obtained with the use of a time series analysis of the lap-based ΔCOM data (NIST/SEMATECH e-Handbook of Statistical Methods, 2003). The average ΔCOM data across 15 laps were lagged by 1 lap, and the autocorrelation coefficient (see the Experimental Procedures) was calculated between the original ΔCOM data and the lagged data. This procedure was repeated for different amounts of lag (1 to 13 lags), which are shown as autocorrelation plots in Figure 3. Autocorrelation plots are commonly used for checking randomness in a time series data set (NIST/SEMATECH e-Handbook of Statistical Methods, 2003). If they are random, such autocorrelations should be near 0 for all time-lag separations, whereas, if they are nonrandom, one or more of the autocorrelations will be significantly nonzero (especially at lag 1). The autocorrelation plots (Figure 3) show a time-dependent trend in the data (e.g., increasing or decreasing pattern in the COM shift); there were obvious downward trends in the ΔCOM in D1-MIS-CA3 and D2-MIS-CA1 (autocorrelation decreasing from positive to negative across lags) and less obvious, yet observable, trends in D3-MIS-CA1 and D4-MIS-CA1. The autocorrelation graphs for other conditions showed random fluctuations with no apparent time-dependent trends, which suggests that there were no time-dependent shifts in the COM in those conditions. The autocorrelation coefficient at lag 1 shows the time-dependent trend most sensitively (NIST/SEMATECH e-Handbook of Statistical Methods, 2003), and there was a significant autocorrelation between the two time series data sets in D1-MIS-CA3 (see lag 1 in Figure 3; autocorrelation coefficient = 0.5; $p < 0.05$). On day 2, the autocorrelation at lag 1 approached significance (D2-MIS-CA3 in Figure 3; autocorrelation coefficient = 0.4; $p = 0.09$) and remained insignificant afterward (autocorrelation coefficient = 0.05, $p > 0.5$ on day 3; autocorrelation coefficient = − 0.03, $p > 0.5$ on day 4). Conversely, no significant autocorrelation at lag 1 was found in D1-MIS-CA1 (Figure 3; autocorrelation coefficient = 0.2; $p > 0.1$), yet a highly significant autocorrelation was observed 24 hr later at lag 1 on day 2 (autocorrelation coefficient = 0.66; $p < 0.01$). The autocorrelations at lag 1 on later days were not significant in CA1 (Figure 3; autocorrelation coefficient = 0.3, $p > 0.1$ on day 3; autocorrelation coefficient = 0.4, $p = 0.1$ on day 4), but the downward trend in the autocorrelation coefficients with increasing lags is apparent, and the last lag (lag 13) showed a significantly negative correlation for days 2–4. It can be concluded that the ΔCOM of a given lap was systematically correlated with the ΔCOM of the previous lap in CA3, but not in CA1, on day 1, and that pattern was reversed between the two subfields in 24 hr.

Lap-by-Lap Skewness and Size of Place Fields in CA3 and CA1

Other major place field parameters that are reported to undergo experience-dependent changes are the skewness and size of the place field, as the fields become more negatively skewed and larger with experience (Mehta et al., 2000). Consistent with this report, the COM shift observed in D1-MIS-CA3 in our study was also accompanied by the development of negative skewness across laps (Figure 4A). A polynomial regression analysis (order 2) in CA3 was significant in D1-MIS ($p < 0.01$). A similar trend was observed only in earlier laps in D2-MIS-CA3 (laps 1–5), after which no significant development of negative skewness across laps was observed in CA3 on day 3 ($p > 0.5$) and day 4 ($p > 0.5$). It is important to note that on days 3 and 4, the place fields in CA3 were negatively skewed from the first lap and remained negatively skewed across most laps. This result may suggest that a long-lasting, underlying plasticity mechanism may have saturated in CA3 after day 2,

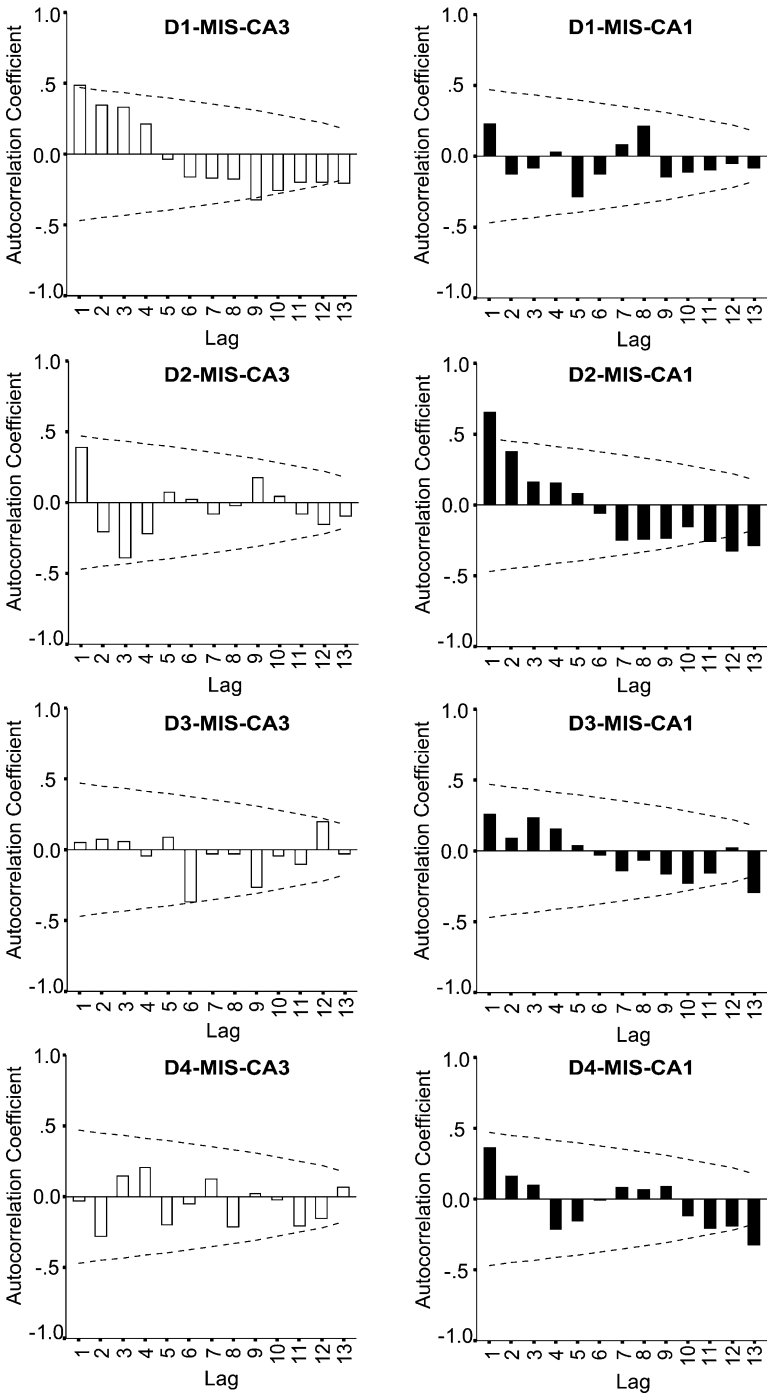

Figure 3. Autocorrelation Coefficient Graphs of the ΔCOM for CA1 and CA3 in the Mismatch Sessions across 4 Days

The abscissa represents the amount of lag that was used to calculate the autocorrelation coefficient between the original ΔCOM data and the lagged ΔCOM data. The ordinate denotes the autocorrelation coefficient between the two data sets. Note the gradual decreases in the amounts of autocorrelation across lags, especially in D1-MIS-CA3 and D2-MIS-CA1, as well as to a lesser degree in D3-MIS-CA1 and D4-MIS-CA1. Dotted lines denote 95% confidence bounds.

causing the place fields to remain maximally skewed from the beginning of the session on the later days and thereby precluding any backward shift of the COM (Figure 2C). The changes in skewness were accompanied by changes in the size of place fields in CA3 across days; the size of the place field significantly increased across 15 laps on day 1 ($p < 0.01$; second-order polynomial regression; also see the first few laps on day 2 in Figure 4B), matching the time course of the development of negative skewness on that day. Little, if any, significant expansion in the place field size was observed across laps on day 3 and day 4 in CA3 (p values > 0.5; regression analysis; Figure 4B).

Interestingly, those place field parameters (i.e., skewness and size) showed more complex patterns of change across days in CA1 in our study (Figure 4; see also Supplemental Figure S3 at http://www.neuron.org/cgi/content/full/42/5/803/DC1) compared to a previous report (Mehta et al., 2000). That is, the negative skewness development was not obvious in CA1 across laps throughout the experiments (p values > 0.2; regression analysis; Figure 4A). The size of CA1 place fields signifi-

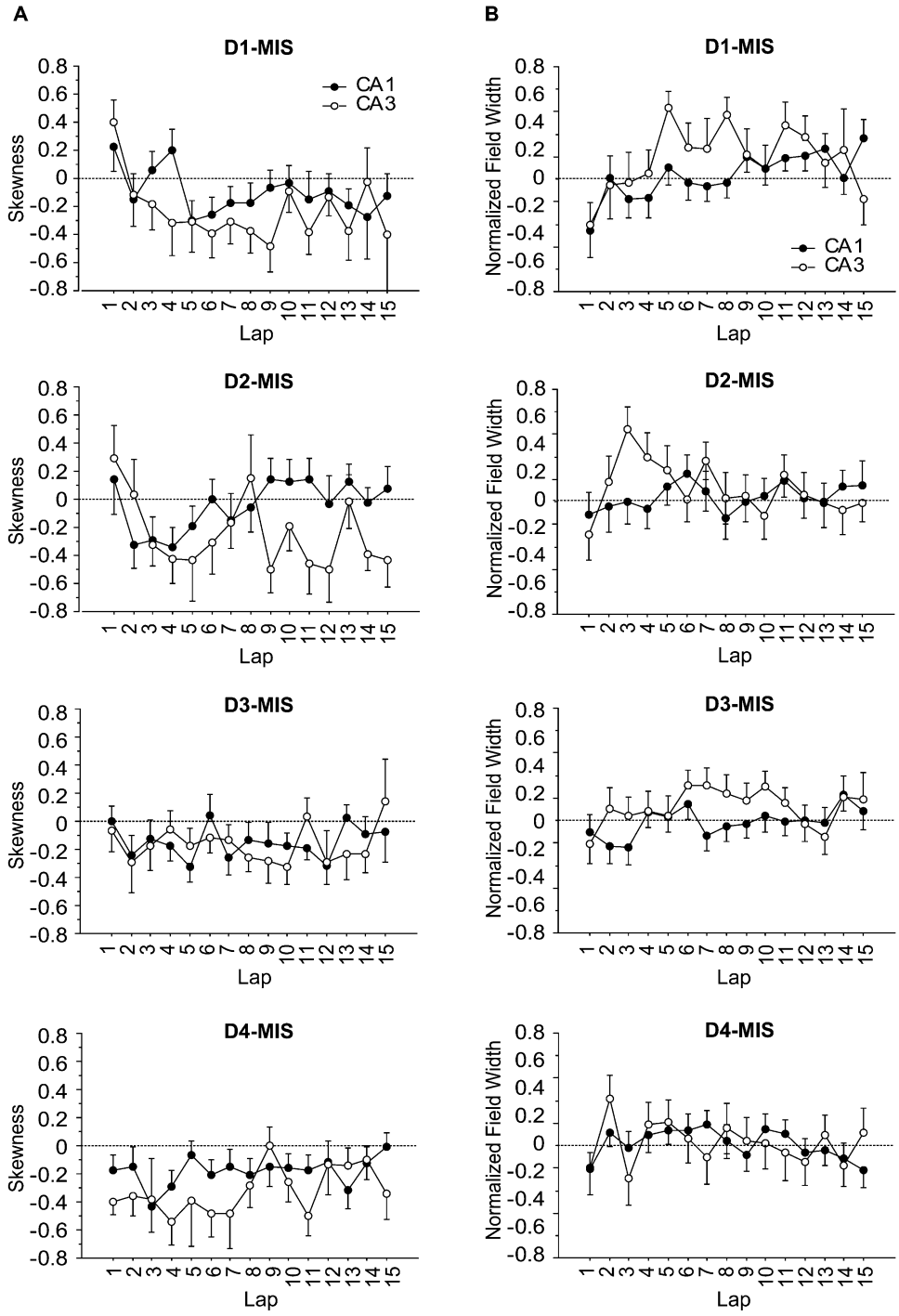

Figure 4. Lap-Based Skewness and Normalized Place Field Size in the Mismatch Sessions

(A) Skewness. Negative skewness means that the place field shape was skewed toward the direction of the rat's movement (CW). Negative skewness was developed across laps in D1-MIS-CA3 and in earlier laps in D2-MIS-CA3 (laps 1–5).

(B) The size of a lap-based place field (normalized by the size of the session-based, average place field). Increases in the field size were noticeable across laps, especially on day 1, in both CA1 and CA3.

cantly increased across laps on day 1 ($p < 0.001$; regression analysis) but did not increase significantly on days 2–4 (Figure 4B).

In sum, the results suggest that the COM shift across laps in CA3 (Figure 2C) during the first mismatch sessions (D1-MIS-CA3) was caused by the development of a negative skewness and the expansion of the field width, which is similar to the pattern of changes observed in CA1 place fields in the previous study (Mehta et al., 2000). In contrast, the COM shift in CA1 was

Table 2. A Comparison of Different Parameters of CA1 and CA3 Place Fields

	STD				MIS			
	CA1		CA3		CA1		CA3	
Mean firing rate (Hz)	1.1	0.1	1.4	0.1	1.2	0.1	1.3	0.1
Maximum firing rate (Hz)	8.7	0.5	8.9	0.8	7.7	0.6	8.0	0.7
In-field firing rate (Hz)	3.9	0.2	3.6	0.2	3.4	0.2	3.4	0.2
Linear field size (°)	66.0	2.0	124.2	6.5	92.2	3.2	132.8	6.5
Integrated field size (°× Hz)	336.6	16.2	429.2	38.3	425.3	26.1	420.7	38.5
Skewness	0.09	0.04	0.35	0.05	0.12	0.04	0.31	0.1

not accompanied by the pattern of changes in the field shape and size that was previously reported by Mehta et al. (2000) (see the Discussion).

Average Size and Skewness of Place Fields in CA3 and CA1

Previous literature showed that the place fields in CA3 mapped more specific regions of space than did the place fields in CA1 (Barnes et al., 1990; Mizumori et al., 1999). We revisited this issue by examining the session-based place fields (i.e., average place fields measured from all 15 laps combined) from both subfields. Interestingly, in the present study, the CA3 place fields mapped a significantly broader region of the track compared to the CA1 place fields; the CA3 place fields represented ~130° of the ring track on average across the standard and mismatch sessions, whereas CA1 place fields mapped ~80° of the track on average (Table 2; Figure 5A). The CA3 place fields were consistently bigger than the CA1 place fields across 4 days (data not shown), suggesting that the observed difference in size was not due to particularly bigger CA3 place fields that might have been recorded on a certain day. Place fields were bigger in mismatch sessions than in standard sessions in both subfields (Table 2; Figure 5A). An ANOVA was performed with the subfield and the cue configuration (i.e., standard or mismatch) as between-group variables; there were significant main effects (p values < 0.0001 for both variables), and there was a significant interaction between the two (subfield cue configuration; $p < 0.05$). A further post hoc analysis showed that the place field size in CA3 was bigger in both standard and mismatch sessions compared to the CA1 place field size (p values < 0.05; Newman-Keuls).

With respect to the average skewness of the session-based place fields (Figure 5B), the place fields in both CA1 and CA3 were significantly skewed negatively in both standard and mismatch sessions ($t = -2.6$, $p < 0.02$ in STD-CA1; $t = -6.7$, $p < 0.0001$ in STD-CA3; $t = -3.0$, $p < 0.01$ in MIS-CA1; $t = -5.7$, $p < 0.0001$ in MIS-CA3; one-group Student's t test). The place fields in CA3, however, were more negatively skewed on average than those in CA1 (Figure 5B); an ANOVA with the subfield and the cue configuration as two between-group variables was performed, and there was a significant main effect of the subfield ($p < 0.0001$). The effect of the cue configuration and the interaction between the main factors (subfield cue configuration) were not significant (p values > 0.1).

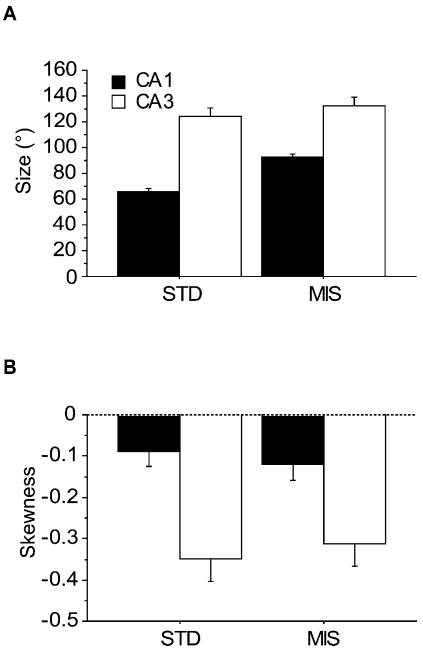

Figure 5. Characteristics of Session-Based, Average Place Fields of CA1 and CA3

(A) Difference in the place field size between CA1 and CA3 averaged for 4 days. Note that the size of the place field of CA3 was consistently bigger in both standard and mismatch sessions.

(B) Skewness of the average place fields in CA1 and CA3 averaged for 4 days. Note that the place fields in CA3 were more negatively skewed in both standard and mismatch sessions.

Discussion

The experience-dependent, backward shift of the COM of CA1 place fields was first reported by Mehta et al. (1997), and subsequent experiments by Ekstrom et al. (2001) showed that systemic injection of the NMDAR blocker -[-]-3-[2-carboxypiperazin-4-yl]-propyl-1-phosphonic acid (CPP) abolished the effect (see also Shen et al., 1997). These results supported a number of computational models that explored how temporally asymmetric long-term potentiation (LTP) and spike timing-dependent plasticity (Levy and Steward, 1983; Magee and Johnston, 1997; Markram et al., 1997) could alter the synaptic connectivity of the hippocampal network to encode learned routes to goal locations as well as more general spatiotemporal representations of behavior (August and Levy, 1999; Blum and Abbott, 1996; Koene et al., 2003; Levy, 1989; Wallenstein et al., 1998). These results have also been interpreted as providing physiological evidence for Hebb's concept of a phase

sequence—that is, a stored set of synaptic weights that cause specific sequences of brain states to be activated, representing temporal sequences of events and allowing predictions of future neural activity based on the present network state (Hebb, 1949; Ekstrom et al., 2001; see also Skaggs and McNaughton, 1996; Louie and Wilson, 2001; Lee and Wilson, 2002).

The present study investigated the COM shift phenomenon in a dynamically changing environment in an effort to dissociate time-dependent plasticity mechanisms in the CA1 and CA3 subfields of the hippocampus (Lee and Kesner, 2002; Nakazawa et al., 2003). Consistent with prior reports (Mehta et al., 1997, 2000), the COM shifted backward in CA1 in a stable, familiar environment (standard sessions; Figure 2B). More importantly, the COM shift was not present in CA3 in the stable, familiar environment, but it appeared strongly in an environment in which the configuration of sensory cues was altered. With respect to its time course, the COM shift occurred in CA3 on the rat's first experience with the altered environment, and it did not appear in CA1 until a day later. These data suggest that the plasticity mechanisms in CA3 are activated immediately in response to the new configurations of sensory landmarks, creating representations of the new spatiotemporal sequences of place cell activity in this altered environment. The plasticity mechanisms in CA1, on the other hand, either were not activated on the first experience with the novel cue configurations or followed a slower time course, such that the backward shift was not apparent until the second day of experience with the novel configurations. These data are consistent with recent behavioral studies that showed that NMDARs in CA3 are necessary for rapid learning of a new environment (Lee and Kesner, 2002) or for one-trial learning of a new goal location (Nakazawa et al., 2003), whereas CA1 NMDARs are necessary for learning on a longer timescale (Lee and Kesner, 2002).

Relationship between COM Shifts and Negative Skewness

Some discrepancies between the present results in CA1 and previous reports are noteworthy. In the present study, CA1 place fields did not exhibit an experience-dependent development of negative skewness (the CA1 fields showed a slight negative skewness on average, but this skewness did not change over laps). Although this result differs from the robust development of negative skewness that was reported by Mehta et al. (2000), it is consistent with the reports of Dragoi et al. (2003) and Huxter et al. (2003), who reported that CA1 place fields in their experiments were not negatively skewed, on average (see also Frank et al., 2002). Although differences in the place field definition criteria may complicate direct comparisons across different investigators, development of negative skewness was also not reported in the original investigation of Mehta et al. (1997; see also Mehta and McNaughton, 1997). That is, strong skewness is not evident in the population data from that experiment, even though a backward expansion and COM shift are clear. Thus, the backward shift of the COM in CA1 is not necessarily accompanied by a development of negative skewness. Theoretically, multiple combinations of different field parameters (e.g., skewness, width, rate, etc.) can result from the hypothesized spike timing-dependent plasticity mechanism, causing the COM of the place field to shift; three possibilities are illustrated in Figure 6. Depending on the precise experimental conditions and spatial cues that are available, in some cases the place field might become negatively skewed; in other cases the place field might expand backward, and the cell might fire at a higher rate, but the field will remain symmetric; and in other cases the field might remain approximately the same size and shift backward. In the present results, the CA1 place fields apparently conformed to the latter description. It remains to be determined what conditions promote different changes in such field parameters as shape and size. Nonetheless, place cells represent backward-shifted locations with experience consistently in different experimental conditions (including the present results and the results of Mehta et al., 1997, 2000), suggesting that the COM may be a more reliable parameter with which to investigate sequence coding mechanisms in the hippocampus.

Long-Term Memory in CA3 versus Novelty Detection in CA1

One puzzling aspect of the COM shifts in CA1 that were reported by Mehta et al. (1997, 2000) was that the potentiated synapses apparently reset back to baseline within a 24 hr period, as the COM shift and the development of negative skewness appeared anew each day. Mehta and McNaughton (1997) suggested that uncorrelated activity in the intervening hours might depotentiate the synapses. Although this is a plausible mechanism to explain the phenomenon, it suggests that CA1 is not the storage site for long-term memories of the learned sequences. The present data suggest that the long-term storage may reside in the CA3 network. CA3 place fields developed negative skewness over the first few laps on days 1 and 2 in the mismatch conditions, and on days 3 and 4 they maintained this negative skewness from the very first lap (Figure 4A). Moreover, CA3 place fields were significantly more skewed than CA1 place fields in both the standard and mismatch sessions (Figure 5B). Thus, the lack of a COM shift in CA3 in the standard environment and after the first day in the mismatch environment may be the result of a saturation of the LTP mechanisms, causing the place fields to become maximally skewed and shifted, without the 24 hr depotentiation that apparently occurs in CA1.

One plausible interpretation for this difference between the regions is that CA1 may need to repeat the potentiation-depotentiation cycle for its synapses to subserve a cognitive function, such as novelty detection in the environment (Figure 7). This interpretation is consistent with many hippocampal models that have emphasized the role of CA1 in detecting novelty, mainly due to its unique anatomical position, which allows it to monitor both the intrahippocampal code that is relayed from CA3 and the cortical sensory information that is relayed mainly from the entorhinal cortex (Blum and Abbott, 1996; Hasselmo and Schnell, 1994; Levy, 1996; Lisman, 1999; Lynch and Granger, 1992). Based on this hypothesis, CA1 may need to reactivate the synaptic plasticity mechanisms for reprocessing the same se-

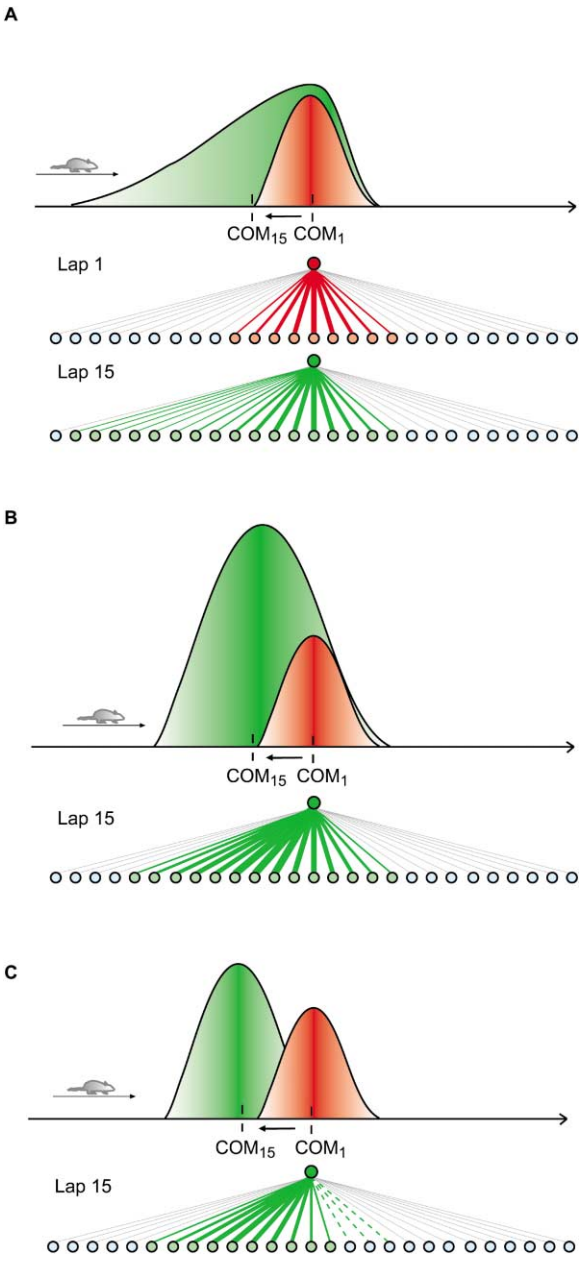

Figure 6. Illustration of Different Ways in which the Shift in the COM of the Place Field May Occur in an Experience-Dependent Manner

(A) (Top) The place field is elongated in the opposite direction relative to the rat's direction of motion. The resulting place field in a later lap (green) is negatively skewed compared to the original place field (red), and the COM is thus shifted backward ($COM_1 \rightarrow COM_{15}$; as in D1-MIS-CA3 in the current study and Mehta et al., 2000). (Middle and bottom) Hypothetical connections among place cells, which may underlie the COM shift of the place field (top). The circles represent place cells, and the lines connecting the circles denote connections from the line of cells at the bottom to the single cell at the top (thicker lines show more potentiated synaptic connections between cells). The postsynaptic place cell produces the place fields that are shown. Synaptic connections between the place cells on the first lap (lap 1; red) are initially symmetric, and as the rat passes through the place field multiple times (e.g., lap 15; green), the synaptic connections are strengthened only between the postsynaptic cell and the presynaptic cells that fired earlier via the temporally asymmetric LTP-induction mechanism, as previously modeled by Mehta et al. (2000).

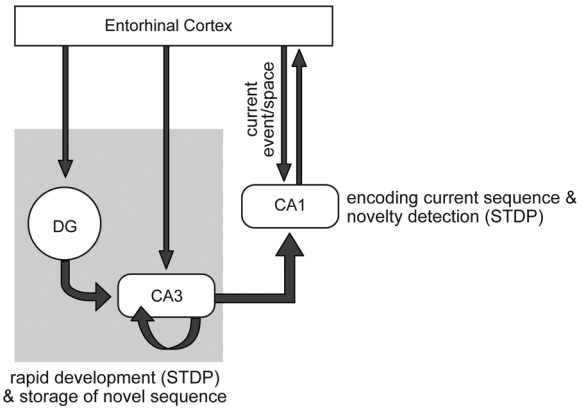

Figure 7. A Model of Sequence Memory Processing in Different Subfields of the Hippocampus

The entorhinal cortex sends current, sensory inputs to the dentate gyrus (DG) and the CA1 and CA3 subfields of the hippocampus. The DG-CA3 network rapidly encodes new spatiotemporal sequence information for long-term storage in the CA3 synaptic matrix. In a familiar environment, the CA1 network encodes the current sequence of locations/events, based on its entorhinal inputs, and compares this sequence with the stored information of the typical (expected) sequences of locations/events in CA3. A significant mismatch between those sequences may trigger a mechanism (e.g., excitation of cholinergic inputs) that reinitiates the encoding process of the novel information in the DG-CA3 network. For simplification, the CA1 output pathway to the entorhinal cortex via the subiculum is omitted. STDP, spike timing-dependent plasticity.

quences of place fields in the familiar environment to detect any novelty that might be encountered in the environment. In other words, based on its entorhinal inputs, CA1 may encode the sequence of places (or events) that the animal is currently experiencing. It may simultaneously compare these sequences with the stored sequences in CA3 that represent the learned patterns that have usually occurred in the animal's past experiences in the environment. If there is a discrepancy between the present sequences and the stored past sequences, this may trigger processes that are adaptive for dealing with a novel environment or novel experiences in the same environment. These processes presumably include the rapid encoding of the new sequences into the CA3 network, perhaps as the result of

(B) (Top) The place field is also elongated in the opposite direction to the rat's motion. However, in this case, no skewness is developed over time, but the same amount of shift in the COM can occur, with the field expanding in the direction opposite to the rat's movement. (Bottom) Stronger potentiation of the connections, compared to those in (A), between the current place cell and the place cells that were activated earlier on the track may maintain the bell shape of the place field while shifting the COM backward.

(C) (Top) The place field maintains its shape and size relatively constant in this example, yet moves its position over time. Although neither skewness nor the size of the place field changes by much, the shift in the COM can occur. (Bottom) Unlike the examples in (A) and (B), this type of COM shift involves a long-term depression (LTD) mechanism in the synaptic connections between the place cells; synaptic connections between presynaptic cells that fire after the postsynaptic cell depress (dashed lines), with concomitant strengthening of connections between presynaptic cells that fire before the postsynaptic cell, as in (A) and (B).

novelty-induced changes in the cholinergic input into the hippocampus (Hasselmo, 1999).

Place Field Size Differences in CA3 and CA1

With respect to the spatial specificity of the place field, previous studies reported that the pyramidal cells in CA3 represented more specific locations of space compared to the CA1 pyramidal cells (Barnes et al., 1990; Mizumori et al., 1999; but see McNaughton et al., 1983). Most computational models have suggested that the CA3 recurrent collateral fiber system allows the embodiment of key computational processes of CA3, such as pattern completion or sequence learning (August and Levy, 1999; Kali and Dayan, 2000; Levy, 1996; Treves and Rolls, 1994; Wallenstein et al., 1998). Therefore, it is possible that the CA3 place fields were larger than those in CA1 in our study mainly because the pyramidal cells in the middle or distal CA3 area of the hippocampus receive the most extensive associational inputs from other CA3 cells (Ishizuka et al., 1990), thus representing broader regions of space compared to the CA3 cells in the hilar area and the cells in CA1. Consistent with this interpretation, Mizumori et al. (1995) showed that, when direct comparisons were made between hilar/CA3 place fields and the more laterally placed CA3 fields, the more lateral CA3 fields were broader (i.e., less spatially specific) than the CA1 and hilar/CA3 fields. It would be important to further investigate this possibility of heterogeneous spatial representations within CA3 (possibly within CA1 as well) by simultaneously monitoring CA3 place cells in the hilar versus middle-distal areas to better understand the detailed organizational rules of spatial representation within the hippocampus.

Implications

The results from the current study present a demonstration of a major difference in the firing properties of place cells in the CA1 and CA3 subfields. Although important physiological differences between CA1 and CA3 have been reported (e.g., Csicsvari et al., 2000, 2003), most place field studies of CA1 and CA3 have failed to show a marked difference in the properties of the areas (aside from some reports of differences in firing rates and mean size of the place fields; Barnes et al., 1990; Mizumori et al., 1995, 1999). Most of these studies have involved recording conditions in which the rat is overtrained to perform the task, such that the hippocampus reaches a steady-state, stable representation of the environment. The present results indicate that the investigation of physiological correlates of the unique, computational functions of the hippocampal subfields will benefit from experimental conditions in which the inputs into the hippocampus are in dynamic flux, such as when the environment is altered, when the rat enters a completely novel environment, or when the behavioral contingencies in an environment are altered (Knierim, 2002; Markus et al., 1995; Mizumori et al., 1999; Moita et al., 2003; Wilson and McNaughton, 1993). Furthermore, previous studies typically recorded cells first in CA1 before electrodes were lowered further to CA3. Such a temporal gap caused by recording the two subfields sequentially would increase the possibility of losing subtle and dynamic differences between CA1 and CA3 that might occur in a limited time frame.

Much recent work on hippocampal function has focused on the role that is played by the hippocampus in episodic memory (Eichenbaum, 2000; Tulving and Markowitsch, 1998; Vargha-Khadem et al., 1997), that is, the memory of specific events that have occurred in a unique spatiotemporal context. Memory for episodic events requires a rapid, one-trial mechanism for acquisition. This type of memory has a spatiotemporal component, as one remembers not only the event itself, but also the spatial context in which it occurred and the temporal order of how the event relates to immediately preceding and subsequent events. The results reported here suggest that the CA3 network may rapidly create representations of such spatiotemporal sequences, which may endow it with a primary role in the rapid formation of episodic memories in humans and analogous types of memories in nonhuman animals.

Experimental Procedures

Subjects and Surgery

Fourteen male Long-Evans rats were maintained at 80%–90% of their ad libitum weights and had free access to water. The rats were housed individually on a reversed 12:12 light/dark cycle, and all the experiments were performed during the dark portion of the cycle. Animal care and all surgical procedures were performed according to National Institutes of Health guidelines and were approved by the University of Texas Health Science Center at Houston Institutional Animal Care and Use Committee.

Each animal was anesthetized (initial dose of 60 mg/kg ketamine and 8 mg/kg xylazine, followed by isoflurane inhalation to effect during surgery), and a microdrive array was implanted over the right dorsal hippocampus (4.2 mm posterior to bregma; 4.5 mm lateral from midline). The microdrive array was composed of either 14 recording probes (Neuro-hyperdrive; Kopf Instruments, Tujunga, CA; eight subjects) or 20 recording probes (using a custom-built hyperdrive; six subjects). Recording probes were tetrodes (Gray et al., 1995; Wilson and McNaughton, 1993) made of four lengths of fine nichrome wire (Rediohm-800, 0.0005 inches; Kanthal, Palm Coast, FL) twisted together and gold plated to reduce the final impedance to 250–500 k measured at 1 kHz (Impedance tester IMP-1; Bak Electronics, Germantown, MD). For detailed descriptions of the recording system, see Knierim (2002).

Training

Following a week of recovery after surgery, the rats were trained to run clockwise (CW) on a circular track (56 cm inner diameter and 76 cm outer diameter) to collect chocolate sprinkles arbitrarily placed on the track by an experimenter. The rats underwent 6 to 21 training sessions over ~7 days (range, 2–12 days) before the beginning of the experiment. The track was positioned inside a black circular curtain (2.7 m diameter) that reached from the ceiling to the floor. Six different objects (distal cues) were hanging on the curtain or standing on the floor at the perimeter of the curtain (hanging cues were a brown cardboard circle, a black-and-white-striped card, and a white card; standing cues were a white box, an intravenous stand with a laboratory coat and a blue cloth, and a roll of brown wrapping paper). The track itself was composed of four different textured surfaces, each covering one-quarter of the ring: a gray rubber mat with a pebbled surface, brown medium-grit sand paper, beige carpet-pad material, and gray duct tape with white tape stripes. Throughout all training sessions, the local cues on the track and the array of distal cues were maintained at a constant configuration (standard configuration). During the training days, the electrodes were advanced gradually over the course of many days to place the electrodes in the vicinity of pyramidal cell layers in CA1 and CA3.

Behavioral Testing

On each testing day, each animal was given a baseline sleep period (30 min), during which multiple cells were recorded, before the first behavioral testing session and after the last testing session. The data that were collected during sleep were used to determine the stability of recordings that were made during behavioral sessions, and unstable cells were not analyzed further. After the first sleep session, the rat was placed in a covered box and was walked briefly around the computer room before entering the adjacent behavior room. The rat was placed on the ring track at an arbitrarily chosen location and finished 15 CW laps for a given session. On a given day, three standard cue configuration sessions were presented. In between those identical standard sessions, the track was rotated counterclockwise (CCW) 22.5°, 45°, 67.5°, or 90°, and the distal cues were rotated CW by an equal amount (Figure 1A). The total amount of mismatch between local and distal cues, therefore, was 45°, 90°, 135°, or 180°. The rats experienced two complete sets of each mismatch amount over 4 days, with each mismatch being run in a pseudorandom order.

Histology

After the completion of experiments, small marker lesions were made on a subset of the tetrode tips 1 day before perfusion. Each animal was perfused transcardially. The frozen brain was cut at 40 μm sections on either a microtome or a cryostat and stained with cresyl violet. Electrode tracks were identified under a light microscope. Each tetrode was then assigned to a hippocampal subfield based on the histological results in addition to the electrophysiological depth profiles that were collected during the experiments. Specifically, digital photomicrographs were taken for all serial sections of the hippocampus (40 μm). Tetrode tracks were traced on the digital images using graphic software (Adobe, San Jose, CA), and those retouched images were reconstructed three-dimensionally (Voxar, Edinburgh, UK). Microscopic examinations were used in parallel in the course of reconstruction. Rotated three-dimensional views of the reconstructed 3D image were compared to the configuration of the tetrodes in the original tetrode bundle for accurate identification of the tetrodes.

Data Analysis

Offline unit isolation was made using custom software running on a PC. The relative amplitudes of signals that were recorded simultaneously at four different wires of the tetrode were primarily used for the isolation of single units. Other parameters of waveforms, such as spike width and height, were also used. Recording stability was assessed visually by comparing patterns of waveform parameter clusters in the two sleep sessions before and after the behavioral sessions each day.

The circular ring track was linearized for the purpose of analysis. The track was divided into 360 bins (1°/bin), and a firing rate for each bin was calculated by dividing the number of spikes that were fired while the rat occupied that bin by the amount of time that was spent in the bin. No smoothing procedure was applied to the place field. The linear size (or width) of a place field (in degrees) was defined by the distance between the field boundaries. Following Mehta et al. (1997), the place field boundaries were defined by the bins in which the mean firing rate fell below 10% of the peak firing rate of the place field for 20 contiguous bins (a lap-based place field was subsequently analyzed within these boundaries only). The spatial information score was calculated according to Skaggs et al. (1993, 1996). Only cells that had a statistically significant ($p < 0.01$) information score of ≥ 0.5 with ≥ 50 spikes were included in the analysis. Skewness was defined as the ratio of the third moment of the place field firing rate distribution divided by the cube of standard deviation (Kirk, 1989; Mehta et al., 2000). The average position of a place field on the track was defined by calculating the COM of the firing rate distribution within the place field boundaries (Mehta et al., 1997, 2000). The width of a lap-based place field was defined by calculating the distance between the first and the last spike positions in the lap (within the boundaries of the overall place field). Calculation of the lap-based field width and the COM was restricted to the laps in which at least two spikes fired. The time series analysis for COM data was performed using the SPSS software package. The formula for the autocorrelation coefficients in this analysis was

$$R_h = \frac{\sum_{t=1}^{N-h} (Y_t - \bar{Y})(Y_{t+h} - \bar{Y})}{\sum_{t=1}^{N} (Y_t - \bar{Y})^2}$$

where h = the time lag (1, 2, 3, ..., 13), N is the total number of laps, and Y is the ΔCOM for the lap (NIST/SEMATECH e-Handbook of Statistical Methods, 2003). A regression analysis (either simple or second-order polynomial) was used throughout the paper to test whether the slope of a curve was significantly positive or negative.

Acknowledgments

We thank Sheri J.Y. Mizumori, Harel Z. Shouval, and D. Yoganarasimha for their valuable comments on the manuscript; and D. Yoganarasimha for assistance in data acquisition. This work was supported by NIH grants RO1 NS29456 and K02 MH63297 and by the Lucille P. Markey Charitable Trust.

Received: November 7, 2003
Revised: March 29, 2004
Accepted: April 22, 2004
Published: June 9, 2004

References

August, D.A., and Levy, W.B. (1999). Temporal sequence compression by an integrate-and-fire model of hippocampal area CA3. J. Comput. Neurosci. *6*, 71–90.

Barnes, C.A., McNaughton, B.L., Mizumori, S.J., Leonard, B.W., and Lin, L.H. (1990). Comparison of spatial and temporal characteristics of neuronal activity in sequential stages of hippocampal processing. Prog. Brain Res. *83*, 287–300.

Blum, K.I., and Abbott, L.F. (1996). A model of spatial map formation in the hippocampus of the rat. Neural Comput. *8*, 85–93.

Csicsvari, J., Hirase, H., Mamiya, A., and Buzsaki, G. (2000). Ensemble patterns of hippocampal CA3-CA1 neurons during sharp wave-associated population events. Neuron *28*, 585–594.

Csicsvari, J., Jamieson, B., Wise, K.D., and Buzsaki, G. (2003). Mechanisms of gamma oscillations in the hippocampus of the behaving rat. Neuron *37*, 311–322.

Dragoi, G., Harris, K.D., and Buzsaki, G. (2003). Place representation within hippocampal networks is modified by long-term potentiation. Neuron *39*, 843–853.

Eichenbaum, H. (2000). A cortical-hippocampal system for declarative memory. Nat. Rev. Neurosci. *1*, 41–50.

Ekstrom, A.D., Meltzer, J., McNaughton, B.L., and Barnes, C.A. (2001). NMDA receptor antagonism blocks experience-dependent expansion of hippocampal "place fields." Neuron *31*, 631–638.

Frank, L.M., Eden, U.T., Solo, V., Wilson, M.A., and Brown, E.N. (2002). Contrasting patterns of receptive plasticity in the hippocampus and the entorhinal cortex: an adaptive filtering approach. J. Neurosci. *22*, 3817–3830.

Gray, C.M., Maldonado, P.E., Wilson, M., and McNaughton, B. (1995). Tetrodes markedly improve the reliability and yield of multiple single-unit isolation from multi-unit recordings in cat striate cortex. J. Neurosci. Methods *63*, 43–54.

Hasselmo, M.E. (1999). Neuromodulation: acetylcholine and memory consolidation. Trends Cogn. Sci. *3*, 351–359.

Hasselmo, M.E., and Schnell, E. (1994). Laminar selectivity of the cholinergic suppression of synaptic transmission in rat hippocampal region CA1: computational modeling and brain slice physiology. J. Neurosci. *14*, 3898–3914.

Hebb, D.O. (1949). The Organization of Behavior: A Neuropsychological Theory (New York: John Wiley & Sons).

Huxter, J., Burgess, N., and O'Keefe, J. (2003). Independent rate and temporal coding in hippocampal pyramidal cells. Nature *425*, 828–832.

Ishizuka, N., Weber, J., and Amaral, D.G. (1990). Organization of intrahippocampal projections originating from CA3 pyramidal cells in the rat. J. Comp. Neurol. *295*, 580–623.

Kali, S., and Dayan, P. (2000). The involvement of recurrent connections in area CA3 in establishing the properties of place fields: a model. J. Neurosci. *20*, 7463–7477.

Kirk, R.E. (1989). Statistics: An Introduction, Third Edition (Fort Worth, TX: Dryden Press).

Knierim, J.J. (2002). Dynamic interactions between local surface cues, distal landmarks, and intrinsic circuitry in hippocampal place cells. J. Neurosci. *22*, 6254–6264.

Koene, R.A., Gorchetchnikov, A., Cannon, R.C., and Hasselmo, M.E. (2003). Modeling goal-directed spatial navigation in the rat based on physiological data from the hippocampal formation. Neural Netw. *16*, 577–584.

Lee, I., and Kesner, R.P. (2002). Differential contribution of NMDA receptors in hippocampal subregions to spatial working memory. Nat. Neurosci. *5*, 162–168.

Lee, I., and Kesner, R.P. (2004). Differential contributions of dorsal hippocampal subregions to memory acquisition and retrieval in contextual fear-conditioning. Hippocampus *14*, 301–310.

Lee, A.K., and Wilson, M.A. (2002). Memory of sequential experience in the hippocampus during slow wave sleep. Neuron *36*, 1183–1194.

Levy, W.B. (1989). A computational approach to hippocampal function. In Computational Models of Learning in Simple Neural Systems, R.D. Hawkins and G.H. Bower, eds. (Orlando, FL: Academic Press), pp. 243–305.

Levy, W.B. (1996). A sequence predicting CA3 is a flexible associator that learns and uses context to solve hippocampal-like tasks. Hippocampus *6*, 579–590.

Levy, W.B., and Steward, O. (1983). Temporal contiguity requirements for long-term associative potentiation/depression in the hippocampus. Neuroscience *8*, 791–797.

Lisman, J.E. (1999). Relating hippocampal circuitry to function: recall of memory sequences by reciprocal dentate-CA3 interactions. Neuron *22*, 233–242.

Louie, K., and Wilson, M.A. (2001). Temporally structured replay of awake hippocampal ensemble activity during rapid eye movement sleep. Neuron *29*, 145–156.

Lynch, G., and Granger, R. (1992). Variations in synaptic plasticity and types of memory in cortico-hippocampal networks. J. Cogn. Neurosci. *4*, 189–199.

Magee, J.C., and Johnston, D. (1997). A synaptically controlled, associative signal for Hebbian plasticity in hippocampal neurons. Science *275*, 209–213.

Markram, H., Lubke, J., Frotscher, M., and Sakmann, B. (1997). Regulation of synaptic efficacy by coincidence of postsynaptic APs and EPSPs. Science *275*, 213–215.

Markus, E.J., Qin, Y.L., Leonard, B., Skaggs, W.E., McNaughton, B.L., and Barnes, C.A. (1995). Interactions between location and task affect the spatial and directional firing of hippocampal neurons. J. Neurosci. *15*, 7079–7094.

McNaughton, B.L., Barnes, C.A., and O'Keefe, J. (1983). The contributions of position, direction, and velocity to single unit activity in the hippocampus of freely-moving rats. Exp. Brain Res. *52*, 41–49.

Mehta, M.R., and McNaughton, B.L. (1997). Expansion and shift of hippocampal place fields: evidence for synaptic potentiation during behavior. In Computational Neuroscience: Trends in Research, J. Bower, ed. (New York: Plenum Press), pp. 741–745.

Mehta, M.R., Barnes, C.A., and McNaughton, B.L. (1997). Experience-dependent, asymmetric expansion of hippocampal place fields. Proc. Natl. Acad. Sci. USA *94*, 8918–8921.

Mehta, M.R., Quirk, M.C., and Wilson, M.A. (2000). Experience-dependent asymmetric shape of hippocampal receptive fields. Neuron *25*, 707–715.

Mizumori, S.J., Garcia, P.A., Raja, M.A., and Volpe, B.T. (1995). Spatial- and locomotion-related neural representation in rat hippocampus following long-term survival from ischemia. Behav. Neurosci. *109*, 1081–1094.

Mizumori, S.J., Ragozzino, K.E., Cooper, B.G., and Leutgeb, S. (1999). Hippocampal representational organization and spatial context. Hippocampus *9*, 444–451.

Moita, M.A., Rosis, S., Zhou, Y., LeDoux, J.E., and Blair, H.T. (2003). Hippocampal place cells acquire location-specific responses to the conditioned stimulus during auditory fear conditioning. Neuron *37*, 485–497.

Nakazawa, K., Sun, L.D., Quirk, M.C., Rondi-Reig, L., Wilson, M.A., and Tonegawa, S. (2003). Hippocampal CA3 NMDA receptors are crucial for memory acquisition of one-time experience. Neuron *38*, 305–315.

NIST/SEMATECH e-Handbook of Statistical Methods. (2003). (http://www.itl.nist.gov/div898/handbook/).

O'Keefe, J., and Dostrovsky, J. (1971). The hippocampus as a spatial map. Preliminary evidence from unit activity in the freely-moving rat. Brain Res. *34*, 171–175.

O'Keefe, J., and Nadel, L. (1978). The Hippocampus as a Cognitive Map (Oxford: Clarendon Press).

Scoville, W.B., and Milner, B. (1957). Loss of recent memory after bilateral hippocampal lesions. J. Neurol. Neurosurg. Psychiatry *20*, 11–21.

Shen, J., Barnes, C.A., McNaughton, B.L., Skaggs, W.E., and Weaver, K.L. (1997). The effect of aging on experience-dependent plasticity of hippocampal place cells. J. Neurosci. *17*, 6769–6782.

Shimizu, E., Tang, Y., Rampon, C., and Tsien, J.Z. (2000). NMDA receptor-dependent synaptic reinforcement as a crucial process for memory consolidation. Science *290*, 1170–1174.

Skaggs, W.E., and McNaughton, B.L. (1996). Replay of neuronal firing sequences in rat hippocampus during sleep following spatial experience. Science *271*, 1870–1873.

Skaggs, W.E., McNaughton, B.L., Gothard, K.M., and Markus, E.J. (1993). An information-theoretic approach to deciphering the hippocampal code. In Advances in Neural Information Processing Systems, S.J. Hanson, J.D. Cowan, and C.L. Giles, eds. (San Mateo, CA: Morgan Kaufman), pp. 1030–1037.

Skaggs, W.E., McNaughton, B.L., Wilson, M.A., and Barnes, C.A. (1996). Theta phase precession in hippocampal neuronal populations and the compression of temporal sequences. Hippocampus *6*, 149–172.

Treves, A., and Rolls, E.T. (1994). Computational analysis of the role of the hippocampus in memory. Hippocampus *4*, 374–391.

Tulving, E., and Markowitsch, H.J. (1998). Episodic and declarative memory: role of the hippocampus. Hippocampus *8*, 198–204.

Vargha-Khadem, F., Gadian, D.G., Watkins, K.E., Connelly, A., Van Paesschen, W., and Mishkin, M. (1997). Differential effects of early hippocampal pathology on episodic and semantic memory. Science *277*, 376–380.

Wallenstein, G.V., Eichenbaum, H., and Hasselmo, M.E. (1998). The hippocampus as an associator of discontiguous events. Trends Neurosci. *21*, 317–323.

Wilson, M.A., and McNaughton, B.L. (1993). Dynamics of the hippocampal ensemble code for space. Science *261*, 1055–1058.